8830 *Inorg. Chem.* **2009**, *48*, 8830–8844
DOI: 10.1021/ic901002y

Inorganic Chemistry
Article

Synthesis, Electronic Structure, and Structural Characterization of the New, "Non-Innocent" 4,5-Dithio-Catecholate Ligand, Its Metal Complexes, and Their Oxidized 4,5-Dithio-*o*-quinone Derivatives

Dimitri Coucouvanis,*,† Alok R. Paital,† Qinwei Zhang,† Nicolai Lehnert,† Reinhart Ahlrichs,‡ Karin Fink,§ Dieter Fenske,∥ Annie K. Powell,∥ and Yanhua Lan∥

†*Department of Chemistry, The University of Michigan, Ann Arbor, Michigan 48109-1055,* ‡*Institute of Physical Chemistry University of Karlsruhe (TH), D-76128 Karlsruhe, Germany,* §*Forschungszentrum Karlsruhe GmbH, Nanotechnology Institute, P.O. Box 3640, D-76021 Karlsruhe, Germany, and* ∥*Institute of Inorganic Chemistry University of Karlsruhe (TH), D-76128 Karlsruhe, Germany*

Received May 23, 2009

The bifunctional ligand catechol-4,5 dithiol, H_2Dtcat, has been synthesized, and the structure of the bis Br^- adduct, $(HS)_2C_6H_2(OH)_2 \cdot 2Ph_4Br \cdot H_2O$, has been determined. The syntheses, molecular structures, electronic structures, and magnetic properties of the monoanionic $[(Dtcat^{2-})_2M]^-$, (M = Ni, **V** and M = Cu, **VI**) complexes have been obtained as Ph_4PBr double salts, $[M(S_2C_6H_2(OH)_2)_2][Ph_4P]_3Br_2$. These and the antiferromagnetically coupled dimeric $[(Dtcat)_2Fe][Ph_4P]_2 \cdot 4DMF$ complex, **VII**, have been structurally characterized. The centrosymmetric $[M(S_2C_6H_2(OH)_2)_2]^-$ complexes in the X-ray isomorphous **V** and **VI** are connected via H-bonding to Br^- ions to form one-dimensional chains well separated from each other by the Ph_4P^+ cations. Magnetic measurements show **V** to be a $S = 1/2$ and **VI** a $S = 0$ molecules. The distribution of electrons in these compounds have been determined by density functional theory calculations which show **V** to be a radical anion Ni(II) complex and **VI** a partially oxidized-ligand, reduced-copper complex. The 4,5 dithio-*o*-quinone $[(Dtoq)_2Ni][Ph_4P]_2$ and $[(Dtoq)_2Cu][Ph_4P]_2$ orthoquinone derivatives of **V** and **VI** have been obtained by oxidation, and their molecular structures have been determined. The dimeric $\{[FeS_2C_6H_2(OH)_2]_2\}^{2-}$ complex, (**VII**) also crystallizes in chains where all OH groups participate in extensive H-bonding. The structure of the dianion **VII** contains S-coordinated Fe(III) ions in a square pyramidal coordination. In **VII**, two low spin Fe(III) ($S = 1/2$) sites are weakly coupled antiferromagnetically with a μ_{eff} of 2.81BM at 270 K and 0.91 BM at 10 K.

Introduction

The definition of non-innocence in ligands has been the subject of numerous discussions. A useful concept is the one that attributes the origin of non-innocence to a similarity in energy of metal orbitals to ligand based redox orbitals.[1,2] In such situations the ambiguity concerning the site of oxidation or reduction within a complex (metal vs ligand) is reflected in electron delocalization. This allows for an expression of the ligand's "non-innocence" in the structural, electronic, and magnetic properties of the metal complexes.

A general class of, structurally similar, non-innocent ligands are the dithiolenes,[3] dioxolenes[4] *o*-phenylene diamines,[5] and other electronically similar ligands.[6] The electronic structures and redox properties of their compounds are unique and have been studied and discussed in detail for many years. Most recently, spectroscopic techniques and sophisticated theoretical calculations, not previously available, have improved greatly our understanding of these compounds.[7,8] A unique

*To whom correspondence should be addressed. E-mail: dcouc@umich.edu.

(1) Ward, M. D.; McCleverty, J. A. *J. Chem. Soc., Dalton Trans.* **2002**, 275–288.
(2) Butin, K. P.; Beloglazkina, E. K.; Zyk, N .V. *Russ. Chem. Rev.* **2005**, *74*, 531–533.
(3) (a) Schrauzer, G. N.; Mayweg, V. *J. Am. Chem. Soc.* **1962**, *84*, 3221. (b) Davison, A.; Edelstein, N.; Holm, R. H.; Maki, A. H. *Inorg. Chem.* **1963**, *2*, 1227. (c) Gray, H. B.; Williams, R.; Bernal, I.; Billig, E. *J. Am. Chem. Soc.* **1962**, *84*, 3596. (d) Ghosh, P.; Bill, E.; Weyhermueller, T.; Neese, F.; Wieghardt, K. *J. Am. Chem. Soc.* **2003**, *125*, 1293. (e) Sun, X. R.; Chun, H.; Hildenbrand, K.; Bothe, E.; Weyhermueller, T.; Neese, F.; Wieghardt, K. *Inorg. Chem.* **2002**, *41*, 4295.
(4) (a) Pierpond, C. G.; Buchanan, R. M. *Coord. Chem. Rev.* **1981**, *38*, 45. (b) Pierpond, C. G.; Lange, C. W. *Prog. Inorg. Chem.* **1994**, *41*, 331. (c) Pierpond, C. G. *Coord., Chem. Rev.* **2001**, *216*, 99. (d) Haga, M.-A.; Dodsworth, E. S.; Lever, A. B. P. *Inorg. Chem.* **1986**, *25*, 447–453.
(5) Herebian, D.; Bothe, E.; Neese, F.; Weyhermueller, T.; Wieghardt, K. *J. Am. Chem. Soc.* **2003**, *125*, 9116.
(6) Ghosh, P.; Bill, E.; Weyhermueller, T.; Wieghardt, K. *J. Am. Chem. Soc.* **2003**, *125*, 3967.
(7) (a) Ray, K.; Petrenko, T.; Wieghardt, K.; Neese, F. *Dalton, Trans.* **2007**, 1552–1566. (b) Bill, E.; Bothe, P.; Chaudhuri, K.; Chlopek, K.; Herebian, D.; Kokatam, K.; Ray, T.; Weyhermueller, T.; Neese, F.; Wieghardt, K. *Chem.—Eur. J.* **2004**, *11*, 204.
(8) Sarangi, R.; George, S. D.; Rudd, D. J.; Szilagyi, R. K.; Ribas, X.; Rovira, C.; Almeida, M.; Hodgson, K. O.; Hedman, B.; Solomon, E. I. *J. Am. Chem. Soc.* **2007**, *129*, 2316.

 Published on Web 08/19/2009

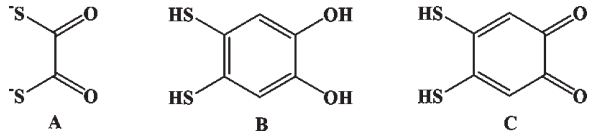

Figure 1. S,S−O,O binucleating ligands.

characteristic of the complexes mentioned above is their strong absorbance in the near IR region of the spectrum. It has been suggested[1] that this low energy high intensity absorbance which is present in some oxidation states and absent in others may make these complexes interesting as electrochromic dyes. Such dyes may find use in the modulation of optical signals transmitted through silica fiber-optics cables. The latter use light in the 1300−1500 nm region where silica is transparent and are of importance in telecommunications.[1] The dithiooxolene-dithiolene "hybrid" molecules/ligands H_2(Dtcat) (Figure 1B), $(Dtcat)^{2-}$, $(Dtcat)^{4-}$, H_2Dtoq (Figure 1C), and $(Dtoq)^{2-}$ are unique and are either redox related or conjugate to each other.

They are expected to display coordination and redox characteristics similar to the non-innocent dithiolenes, or dioxolenes. More importantly, their potential heteronucleating properties should be similar to the dithiooxalate ligand (Figure 1A) and allow for the synthesis of heteronuclear aggregates.

In the past,[9−11] we developed the intriguing chemistry of the dithiooxalate ligand[10] (Dto^{2-}), (Figure 1A), and we explored the use of $[M(Dto)_n]^{n-}$ complexes as ligands for other metal ions (M′). In the $[M(Dto)_n]M'$ complexes the coordination mode of the bridging Dto^{2-} ligand (S−S vs O−O for M or M′) was dictated by thermodynamic and kinetic considerations.[10] In these early studies we demonstrated that it was indeed possible to assemble molecular aggregates or extended lattices.[10b] Our investigations of the $[M(Dto)_n]M'$ complexes and polymers often were hampered by the oxidative instability of the $[M(Dto)_n]^{n-}$ complexes, (M = Cu, Fe), inherent in the Dto ligand, and manifested in its irreversible, two electron, oxidative degradation to S=C=O[9b,11] (eq 1).

$$[Cu^{II}(Dto)_2]^{2-} - e^- \rightarrow [Cu^{III}(Dto)_2]^- \\ + h\nu \rightarrow [Cu^{I}(Dto)(COS)_2]^- \qquad (1)$$

The dithiolene/dioxolene "hybrid"molecules (Figure 1) are robust bifunctional ligands structurally analogous to Dto. Until now the "parent" dithiocatechol (Figure 1B) was not known. The 4,5 dithio-*o*-quinone, H_2Dtoq, (Figure 1C) may be obtained by oxidation/deprotonation of the 4,5-dithio catechol, H_2Dtcat, (**I**), (Figure 1B). The deprotonated form of H_2Dtoq is expected to be more stable but functionally similar to the Dto ligand, (Figure 1A). In this paper we report on the synthesis and structure of (**I**), obtained as a Ph_4PBr double salt, $[Ph_4PBr^-]_2H_2Dtcat\cdot H_2O$, the $[M(Dtcat)_2][Ph_4P]_3Br_2$, (M = Ni, (**V**); M = Cu, (**VI**)), complexes (also obtained as Ph_4PBr double salts), the dimeric $[Fe(Dtcat)_2]_2[Ph_4P]_2\cdot 4DMF$ complex (**VII**) and the $[Ni(Dtoq)_2][Ph_4P]_2$ (**VIII**) and $[Cu(Dtoq)_2][Ph_4P]_2$, (**IX**) complexes (derivatives of H_2Dtoq (Figure 1C)).

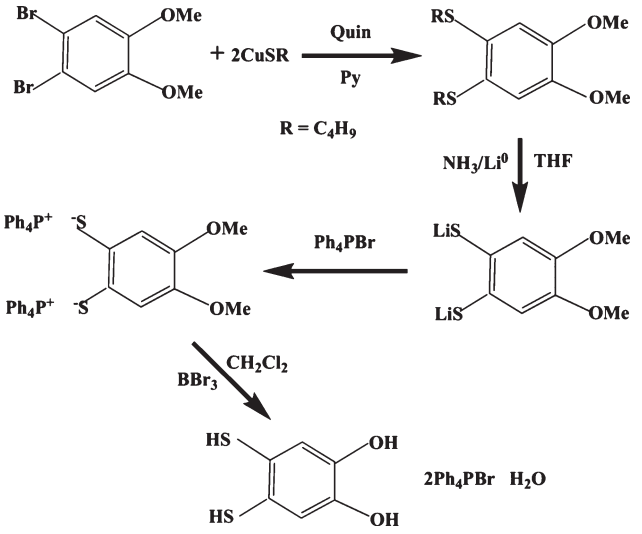

Figure 2. Synthesis of 4,5-dimercapto catechol.

Numbering and Abbreviations Used

numbering	formula	abbreviation
	$[(S_2C_6H_2(OH)_2]^{2-}$	Dtcat
	$(S_2C_6H_2O_2)^{2-}$	Dtoq
I	$(HS)_2C_6H_2(OH)_2\cdot 2Ph_4PBr\cdot H_2O$	H_2Dtcat
V	$Ni(S_2C_6H_2(OH)_2\cdot(Ph_4P)_3Br_2$	$Ni(Dtcat)_2$
VI	$Cu(S_2C_6H_2(OH)_2\cdot(Ph_4P)_3Br_2$	$Cu(Dtcat)_2$
VII	$[Fe(S_2C_6H_2(OH)_2)_2]_2\cdot(Ph_4P)_2\cdot 4DMF$	$[Fe(Dtcat)_2]_2$
VIII	$Ni(S_2C_6H_2O_2)_2(Ph_4P)_2$	$Ni(Dtoq)_2$
IX	$Cu(S_2C_6H_2O_2)_2(Ph_4P)_2$	$Cu(Dtoq)_2$

Results and Discussion

Syntheses and Solution Properties. The synthesis of I (Figure 2) from 4,5 dibromoveratrole is based on modification of published synthetic procedures.[12,13] 1,2-Bis(*n*-butylthio)-4,5- dimethoxybenzene,[12] **II**, was obtained in 55% yield, as an off-white crystalline product, by the reaction of copper(I) butanethiolate[12] and 4,5 dibromoveratrole in a 3:1 quinoline/pyridine mixture. The reaction of **II** in a liquid ammonia/tetrahydrofuran mixture with Li metal affords the off-white dilithium salt of 1,2-dithio-4,5-dimethoxy benzene, **III.**

The cleavage of the C−S bond in liquid ammonia by alkali metals is a well-known reaction.[13] **III** can be isolated as a yellow ditetraphenylphosphonium salt, **IV**, by a cation metathesis reaction. Demethylation of **IV** was carried out in dichloromethane solution using BBr_3 in a manner analogous to the one used previously in the demethylation of 1,2-diamino 4,5-dimethoxybenzene.[14] Pink crystals of bis-tetraphenylphosphonium bromide-4,5-dithio catechol, **I**, were obtained with one water of hydration in 58% yield.

(9) (a) Coucouvanis, D. *J. Am. Chem. Soc.* **1970**, *92*, 707. (b) Coucouvanis, D. *J. Am. Chem. Soc.* **1971**, *93*, 1786. (c) Coucouvanis, D.; Piltingsrud, D. *J. Am. Chem. Soc.* **1973**, *95*, 5556.

(10) (a) Coucouvanis, D. In *Transition Metal Chemistry*; Mueller, A., Diemann, E., Eds.; *Verlag Fur Chemie*, 1981. (b) Hollander, F.; Leitheiser, M.; Coucouvanis, D. *Inorg. Chem.* **1977**, *16*, 1615.

(11) (a) Imamura, T.; Ryan, M.; Gordon, G.; Coucouvanis, D. *J. Am. Chem. Soc.* **1984**, *106*, 984. (b) Kanatzidis, M. G.; Baenziger, N. C.; Coucouvanis, D. *Inorg. Chem.* **1985**, *24*, 2680.

(12) Lowe, N. D.; Garner, C. D. *J. Chem. Soc., Dalton Trans.* **1993**, 2197.

(13) (a) Adams, R.; Ferretti, A. *J. Am. Cem. Soc.* **1959**, *81*, 4927. (b) Adams, R.; Ferretti, A. *Org. Synth.* **1962**, *42*(22), 54.

(14) Rosa, D. T.; Reynolds, R. A., III; Malinak, S. M.; Coucouvanis, D. *Inorg. Synth.* **2002**, 33 112.

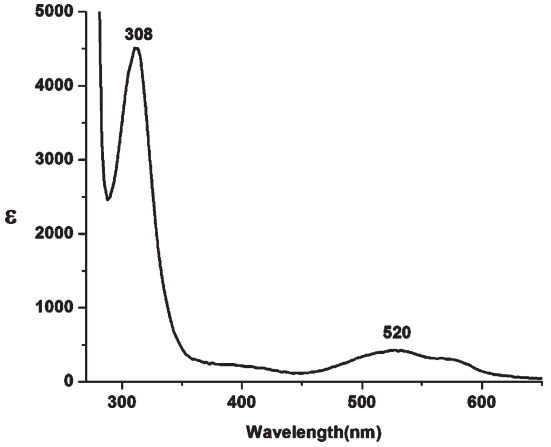

Figure 3. Electronic absorption spectrum of $H_2Dtcat \cdot 2PPh_4Br \cdot H_2O$, **I**, in DMF solution.

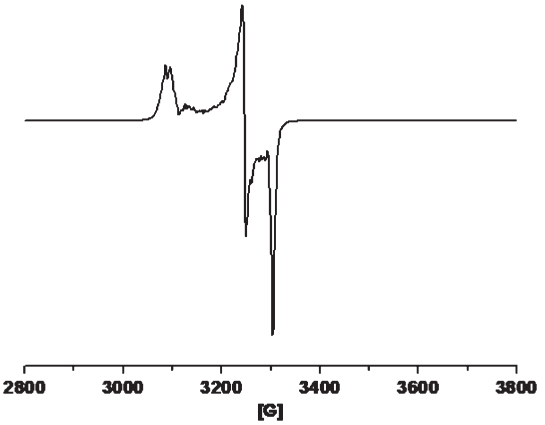

Figure 4. EPR spectrum of the $[Ni(Dtcat)_2]^-$ complex, **V**, (X-band) in DMF glass at liquid N_2 temperature (g values: 2.003, 2.039, 2.136).

The pink color of **I** (Figure 3) is due to a weak absorption at 520 nm (ε = 400) .

Reactions of **I** with $Ni(OAc)_2 \cdot 4H_2O$, $Cu(OAc)_2 \cdot 2H_2O$, and $Fe(OAc)_2$ in *N*,*N*-dimethylformamide (DMF) solution in a 2:1 **I** to metal ratio give the $[Ni(Dtcat)_2]^-$, (**V**), $[Cu(Dtcat)_2]^-$, (**VI**), and $\{[Fe(Dtcat)_2]_2\}^{2-} \cdot 4DMF$, (**VII**), complexes, respectively, which are isolated in crystalline form from DMF solutionas. A fresh solution of **V** (in DMF) is reasonably stable and shows a characteristic electron paramagnetic resonance (EPR) absorption (Figure 4) and an intense electronic absorption at 1015 nm (Figure 5A, Table 1). Upon standing in air this solution slowly becomes EPR silent and shows a change in the electronic spectrum with a strong absorption emerging at 800 nm. (Figure 5B)

This change is much faster (ca. 2 h) in the presence of base (Et_3N). Crystals of this oxidized compound have been obtained and characterized as $(Ph_4P)_2[Ni(Dtoq)_2]$, **VIII**. The high intensity, low energy electronic absorption in the spectrum of **V** is similar to absorptions of other monoanionic bis dithiolene Ni complexes.[15]

Solutions of **VI** in DMF are EPR silent. Upon standing in air the color of these solutions (Figure 6) changes from light green to brown, (Figure 7) and an EPR signal appears rapidly, (Figure 8). As observed previously for **V**, the change is much faster (ca. 30 min) in the presence of base (Et_3N). Crystals of oxidized compound **VI** have been obtained and structurally and chemically characterized as $(Ph_4P)_2[Cu(Dtoq)_2]$, **IX**. The EPR signal of **IX** (Figure 8) is characteristic of Cu(II).

The synthesis of the ortho-quinone derivative of ligand, H_2Dtoq, is non-trivial because of the tendency of **I** to undergo oxidation to polymeric intractable disulfides.

The low temperature, *N*-bromosuccinimide oxidation method[16] failed to produce the *o*-quinone derivative of **I**. The low temperature oxidation of the coordination "protected" S,S chelated ligands in **V**, using *N*-bromosuccinimide,[16] was successful however and gave **VIII** (the ortho-quinone derivative of **V**).

The structural details of the X-ray isomorphous **VIII** and **IX** (vide infra, Table 2) are as expected for the bis dithiolene-*o*-quinone complexes of Ni(II) and Cu(II). The analytical data, diamagnetic nature of **VIII**, the magnetic moment of **IX** (1.85 BM), and the very short C−O bonds in **VIII** and **IX** (Table 3) also are consistent with the *o*-quinone description. At present we can only speculate that oxidation of the, formally M(III), **V** and **VI** complexes followed by dissociation of two catechol protons leads to rapid intramolecular electron transfer and formation of two, formally M(III)-coordinated, dithiolene radicals (Figure 9C). These two-electron oxidized/deprotonated **V** (or **VI**), which also could be described as dithiocatechol-dithioorthoquinone complexes of M(III) (Figure 9D), undergo subsequent one-electron/two-proton loss that leads to the M(II) bis-*o*-quinone complexes **VIII** and **IX** (Figure 9E). A precedent for this reaction exists in the one-electron oxidation of the $(Bipy)_2Ru^{III}$(subcat) complex to the *o*-quinone product $(Bipy)_2Ru^{II}$(subo-q) (where subcat = the 1,2-diolate-anthroquinonato ligand)[17] and also in the photochemically assisted oxidation of the $[Cu(Dto)_2]^{2-}$ complex (eq 1). The description of **V** as a Ni(III) complex (Figure 9A) is only a "book-keeping" formalism. As suggested previously and also on the basis of our density functional theory (DFT) calculations (vide infra) **V** is best described as Ni(II) coordinated to a radical ligand (Figure 9B).

The cyclic voltammetry of **V** and **VI** (in DMF solution vs Ag/AgCl; Figure 10A,B) shows reversible reductions at −0.77 V and −0.76 V, respectively. The cyclic voltammetry of **VII** (Figure 10C) shows a reversible reduction at −1.05 V and a reversible oxidation at 0.092 V. The latter accounts for the rapid air oxidation of violet DMF solutions of **VII** (Figure 11) which assume a green color with emerging absorptions at 669, 592, 415, and 313 nm.

The $[(Dtoq)_2Cu]^{2-}$ dianion, **IX**, undergoes reversible oxidation (Figure 10D). The corresponding Ni(II) complex (**VIII**) undergoes only what can be described as poorly defined, irreversible oxidations. Chemical oxidations of **VIII** and **IX** with $Fe(Cp)_2^+$ in DMF solution gave the same product which, tentatively, has been characterized by elemental analysis as the neutral $(C_6H_2O_2)_2S_3$ trisulfide. On the voltammetry time scale **IX** reversibly gives a "Cu(III)" product. In solution this

(15) Ray, K.; Weyhermiller, T.; Neese, F.; Wieghardt, K. *Inorg. Chem.* **2005**, *44*, 5345.
(16) Marino, J. P.; Schwartz, A. *J. Chem. Soc., Chem. Commun.* **1974**, 812.
(17) DelMedico, A.; Dodsworth, E. S.; Lever, A. B. P.; Pietro, W. J. *Inorg. Chem.* **2004**, *43*, 2654.

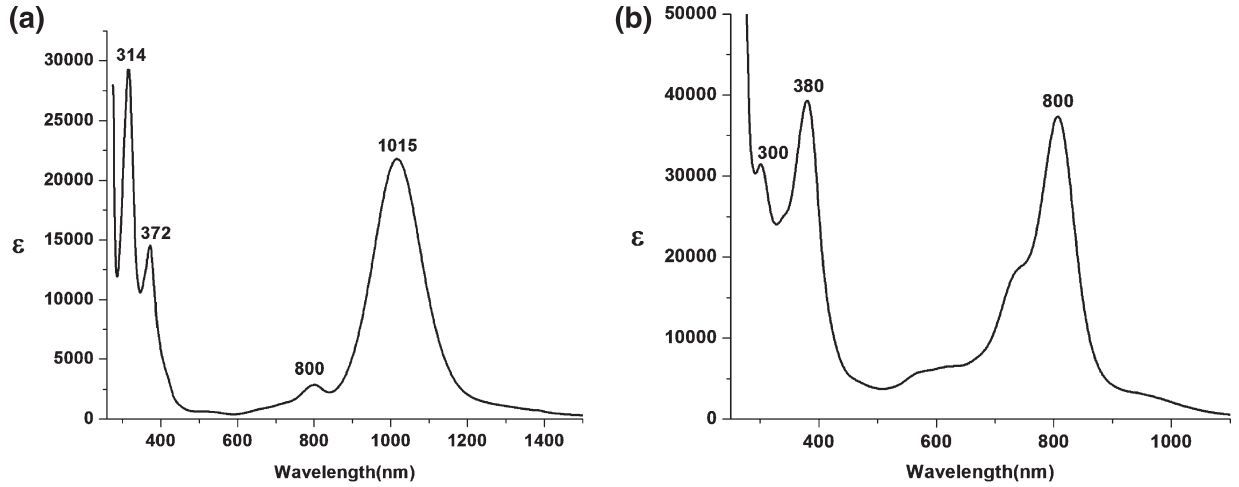

Figure 5. Electronic absorption spectra of (a), $[Ni(Dtcat)_2][Ph_4P]_3Br_2$, **V**, and (b), $[Ni(Dtoq)_2][Ph_4P]_2$, **VIII**, in DMF solution.

Table 1. Electronic Spectra of the Complexes in DMF Solution

compound	color	λ_{max}	ε
I $[H_2Dtcat]\,[Ph_4PBr]_2\cdot H_2O$	pink	520	400
		308	4,500
V $[Ni(Dtcat)_2][Ph_4P]_3Br_2$	greenish-brown	1015	21,750
		800	2,950
		372	14,300
		314	28,600
VI $[Cu(Dtcat)_2][Ph_4P]_3Br_2$	green	630	850
		392	26,550
		341	17,500
VII $[Fe(Dtcat)_2]_2[Ph_4P]_2\cdot 4DMF$	violet	577	7,100
		511	10,600
		384	19,770
		332	17,750
VIII $[Ni(Dtoq)_2][Ph_4P]_2$	green	800	37,300
		380	39,300
		300	31,200
IX $[Cu(Dtoq)_2][Ph_4P]_2$	brown	495	42,900
		471	43,100
		326	10,800

product decomposes to what appears to be the"metal-free" trisulfide derivative of the ligand. At present we have not established whether the ligand undergoes a photochemically induced oxidation.

The X-ray crystal and molecular structure of **I** shows the ligand in two opposing orientations located at $^1/_2$ occupancy around a center of symmetry (Figure 12) and is accompanied by two Ph_4PBr of crystallization and a water molecule. The Br^- anions (at four positions at $^1/_2$ occupancy) and the water molecule connect the $(HS)_2C_6H_2(OH)_2$ molecules via H-bonding. The C−O and C−S distances in **I** (Table 3) are typical of single bonds. The Br^- anions are located close to the ligand and are H-bonded to the catechol hydroxyl groups. The positional disorder of the ligand and the close proximity of several atoms did not allow for the anisotropic refinement of these atoms.

Single crystal X-ray structure determinations show the isomorphous, monoanionic, sulfur chelated, Ni and Cu complexes, **V** and **VI** respectively, to be four-coordinate and planar. They are "double-salts" and contain 2 Ph_4PBr per monoanion in addition to the Ph_4P^+ counterion. In the lattice the centrosymmetric $[M(Dtcat)_2]^-$ complexes (Figure 13) are connected via H-bonding to Br^- ions to form one-dimensional (1-D) chains (Figures 13 and 14) well separated from each other by the Ph_4P^+ cations.

The structural details of **V** and **VI** (Table 3) are similar to those of other monoanionic dithiolene complexes of Ni and Cu such as $[NiS_2C_2(CN)_2]^-$[17,18] and $[Ni(L^{t\text{-}Bu})(L^{t\text{-}Bu}\cdot)_2]^-$[19b] ($L^{t\text{-}Bu}$ = 3,5 di-*tert*-butyl dithiolate). The latter show Ni−S bond lengths of 2.146(1) Å and 2.145(1) Å, respectively, and are 0.2 Å shorter than the Ni−S bond in the $[NiS_2C_2(CN)_2]^{-2}$ dianion at 2.175(1)Å.[18d] A structure determination of V at 300 K shows Ni−S bond lengths very nearly identical to those obtained from the low temperature (Liquid N_2) structure determination. (Table 3, see also Figure 20).

The dimeric $\{[Fe(Dtcat]_2)_2\}^{2-}$ complex, (**VII**), also crystallizes in chains where all OH groups participate in extensive H-bonding mediated by the DMF molecules of solvation (Figure 15). The structure of the dianion is similar to that of the $\{[FeS_2C_2(CN)_2]_2\}^{2-}$ complex[20] and contains a S-coordinated Fe(III) in a square pyramidal coordination. Metrical details (Table 3) include Fe−S distances of 2.2251 Å (range 2.2176(8)−2.2318(8)Å), an intradimer Fe−Fe distance of 3.129(1)Å, and an intradimer Fe−S distance of 2.4726(8)Å. They are similar to those found in the structure of the dimeric $[FeS_2C_2(CN)_2]_2^{-2}$ complex with Fe−S, Fe−Fe, and Fe−S′ distances of 2.23(1), 3.068, and 2.46(1), respectively.[20]

Dithio-orthoquinone Complexes. A fresh solution of **V** (in DMF) is reasonably stable and shows a characteristic EPR absorption (Figure 4) and an intense electronic absorption at 1015 nm (Figure 5A). Upon standing in air this solution slowly becomes EPR silent and shows a change in the electronic spectrum with a strong absorption emerging at 800 nm. (Figure 5B) This change is much faster (ca. 2 h) in the presence of base (Et_3N). Single crystals of this oxidized compound, $(Ph_4P)_2[Ni(Dtcat)_2]$, **VIII**, have been obtained, and the crystal/molecular structure has been determined, (Figure 16, Table 3). The low temperature oxidation of the S,S chelated ligand in

(18) (a) McCleverty, J. A. *Prog. Inorg. Chem.* **1968**, *10*, 49. (b) Schrauzer, G. N. *Transition Met. Chem.* (*N. Y*) **1968**, *4*, 299. (c) Holm, R. H.; Olanov, M. J. *Prog. Inorg. Chem.* **1971**, *14*, 241. (d) Eisenberg, R. *Prog. Inorg. Chem.* **1970**, *12*, 295.

(19) (a) Sellmann, D.; Geck, M.; Knoch, F.; Ritter, G.; Dengler, J. *J. Am. Chem. Soc.* **1991**, *113*, 3819. (b) Sellmann, D.; Binder, H.; Haussinger, D.; Heinemann, F. W.; Sutter, J. *Inorg. Chim. Acta* **2000**, *300*−*302*, 829.

(20) Hamilton, W. C.; Bernal, I. *Inorg. Chem.* **1967**, *6*, 2003.

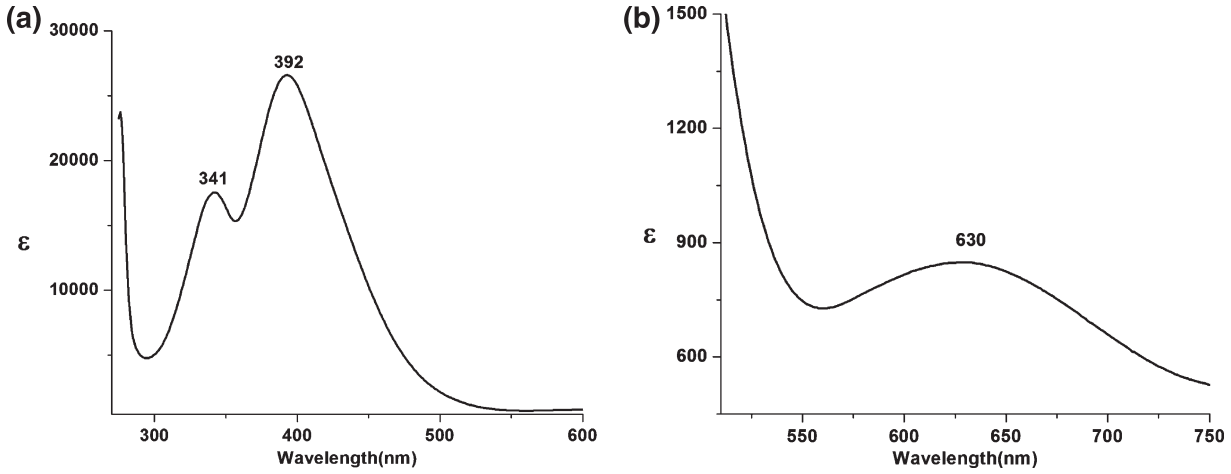

Figure 6. Electronic absorption spectra of $[Cu(Dtcat)_2][Ph_4P]_3Br_2$, **VI**. (a) The charge transfer region and (b) the lower energy d-d region in DMF solution.

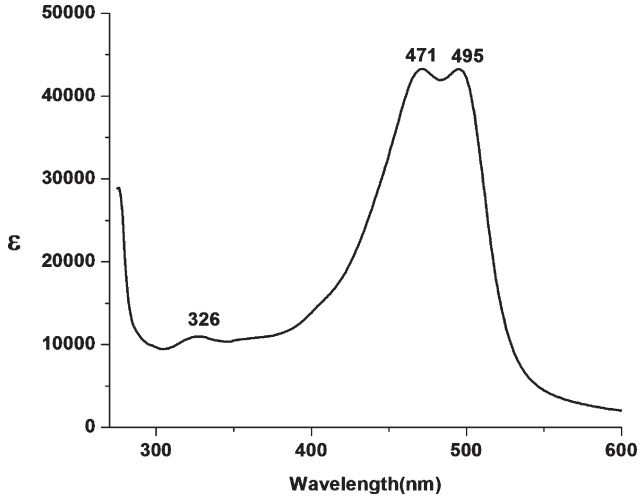

Figure 7. Electronic absorption spectra of DMF $[Cu(Dtoq)_2][Ph_4P]_2$, **IX**, in DMF solution.

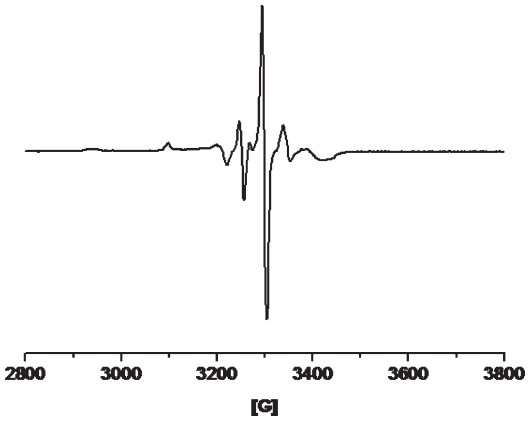

Figure 8. EPR spectrum of **IX**, (X-band) in frozen solution.

V using *N*-bromosuccinimide,[16] also gives **VIII**, the ortho-quinone derivative of **V**. Brown crystals of the X-ray isomorphous, isostructural, complex, $(Ph_4P)_2[Cu(Dtoq)_2]$, (**IX**) also have been isolated in a similar manner from **VI**, and the structure of **IX** has been determined, (Figure 16, Table 3)

Magnetic Properties. In recent years, the electronic structures of dithiolene complexes in unusual formal oxidation levels have been examined in great detail by Wieghardt and co-workers.[22] These studies have further refined and advanced our level of understanding of these molecules that have received attention numerous times[18,22,23] over the last 40 years. Complexes **V**, **VI**, **VII**, **VIII**, and **IX** are new entries in dithiolene chemistry.

The magnetic moment of **V**, at high temperatures, originally appeared lower than expected. It appears that the diamagnetic correction could not be compensated using the Pascal constants[34] calculated for the organic components, ($\chi_{dia} = -5.0 \times 10^{-4}$ cm^3 mol^{-1}). A more accurate diamagnetic correction was anticipated from the diamagnetic **VI** which is isomorphous and isostructural to **V**. From the Curie−Weiss fit in the full temperature range (see above), the diamagnetic contribution for this compound is -1.6×10^{-3} cm^3 mol^{-1}.[24] The magnetic data corrected for diamagnetism using the value -1.6×10^{-3} cm^3 mol^{-1} gives a RT susceptibility of 0.60 cm^3 K mol^{-1} (2.19 μ_B). With either the Pascal's constants diamagnetic corrections, or the correction obtained from **VI**, the χT product decreases at low temperatures to reach a value of 0.34 cm^3 K mol^{-1} at 1.8 K, (Figure 17) indicating the presence of one $S = 1/2$ spin in the system. The 0.34 cm^3 K mol^{-1} value is slightly lower than an anticipated spin only S = 1/2 ground state (expected[25] to be about 0.375 cm^3 K mol^{-1}) and possibly is due to weak intermolecular exchange interactions facilitated by O−H−Br bonding (Figure 17). Magnetic data collected

(21) Kanatzidis, M. G.; Baenziger, N. C.; Coucouvanis, D. *Inorg. Chem.* *24* **1985**, 2680.

(22) (a) Chun, H.; Verani, C. N.; Chaudhuri, P.; Bothe, E.; Weyhermueller, T.; Bill, E.; Wieghardt, K. *Angew. Chem., Int. Ed.* **2001**, *40*, 2489. (b) Bachler, V.; Olbrich, G.; Neese, F.; Wieghardt, K. *Inorg. Chem.* **2002**, *41*, 4179. (c) Ray, K.; Weyhermueller, T.; Goossens, A.; Craje, M. W. J.; Wieghardt, K. *Inorg. Chem.* **2003**, *42*, 4082.

(23) (a) Baker-Hawkes, M. J.; Billig, E.; Gray, H. B. *J. Am. Chem. Soc.* **1966**, *88*, 4870. (b) Williams, R.; Billig, E.; Waters, H.; Gray, H. B. *J. Am. Chem. Soc.* **1966**, *88*, 43.

(24) From the Curie−Weiss fit of the data obtained for **VI**, in the full temperature range, the diamagnetic contribution for this compound is -1.6×10^{-3} cm^3 g^{-1}. A change in the diamagnetism of **VI** with temperature indicates the presence of a small amount of paramagnetic impurity (most likely the $[Cu(Dtoq)_2]^{2-}$ complex, **IX**. The EPR spectrum of **VI** indeed shows a small amount of an $S = 1/2$ signal.

(25) Song, Y.; Gamez, P.; Roubeau, O.; Lutz, M.; Spek, A. L.; Reedijk, J. *Eur. J. Inorg. Chem.* **2003**, 2924–2928.

Table 2. Details Concerning X-ray Data Collection and Structure Refinement of **I**, **V**, **VI**, **VII**, **VIII**, and **IX**

$[Ph_4PBr]_2$ $[Dtcat]\cdot H_2O$	$[(Dtcat^2)_2Cu][Ph_4P]_3Br_2$		$[(Dtoq)_2Cu][Ph_4P]_2$		
	$[(Dtcat^2)_2Ni][Ph_4P]_3Br_2$		$[(Dtcat^2)_2Fe]_2[Ph_4P]_2\cdot 4DMF$		$[(Dtoq)_2Ni][Ph_4P]_2$
I	**V**	**VI**	**VII**	**IX**	**VIII**
pink	brown	green	black	green	green
block	plate	plate	block	block	block
0.34 × 0.28 × 0.24	0.35 × 0.20 × 0.07	0.36 × 0.28 × 0.24	0.37 × 0.27 × 0.22	0.35 × 0.25 × 0.15	0.23 × 0.12 × 0.12
$C_{54}H_{48}Br_2O_3P_2S_2$	$C_{84}H_{68}Br_2NiO_4P_3S_4$	$C_{84}H_{68}Br_2CuO_4P_3S_4$	$C_{84}H_{84}Fe_2\ N_4O_{12}P_2S_8$	$C_{60}H_{44}CuO_4P_2S_4$	$C_{60}H_{44}NiO_4P_2S_4$
1030.84	1581.12	1586.98	1771.75	1082.75	1077.89
triclinic	monoclinic	monoclinic	triclinic	monoclinic	monoclinic
$P\bar{1}$	$P2_1/c$	$P2_1/c$	$P\bar{1}$	$P2_1/n$	$P2_1/n$
10.0956(7)	18.3511(14)	18.4277(14)	11.6061(13)	10.7056(6)	10.7256(6)
10.1702(7)	14.3261(11)	14.2991(11)	13.5992(15)	14.7061(8)	14.6763(8)
11.9686(8)	27.677(2)	27.646(2)	14.7055(17)	15.9161(8)	15.8167(8)
97.3930(10)	90.00	90.00	113.5680(10)	90.00	90.00
103.5190(10)	93.1770(10)	92.9890(10)	102.150(2)	92.1680(10)	92.1330(10)
95.8200(10)	90.00	90.00	96.214(2)	90.00	90.00
1173.82(14)	7265.1(10)	7274.7(9)	2031.3(4)	2504.0(2)	2488.0(2)
1	4	4	1	2	2
85(2)	85(2)	85(2)	85(2)	85(2)	85(2)
1.928	1.600	1.632	0.667	0.717	0.672
520	3244	3248	922	1118	1116
1.77−26.37	1.11−20.82	1.11−20.81	1.57−26.37	1.89−26.37	1.89−26.37
4798	7609	7620	8308	5132	5096
$-12 < h < 12$	$-18 < h < 18$	$-18 < h < 18$	$-14 < h < 14$	$-13 < h < 13$	$-13 < h < 13$
$-12 < k < 12$	$-14 < k < 14$	$-14 < k < 14$	$-16 < k < 16$	$-18 < k < 18$	$-18 < k < 18$
$-14 < l < 14$	$-27 < l < 27$	$-27 < l < 27$	$-18 < l < 18$	$-19 < l < 19$	$-19 < l < 19$
0.0392, 0.1056	0.0287, 0.0707	0.0498, 0.1162	0.0423 0.1140	0.0282, 0.0773	0.0306, 0.0784
0.0413,0.1071	0.0347, 0.0764	0.0530, 0.1187	0.0578, 0.1276	0.0299, 0.0790	0.0364, 0.0825
1.037	1.063	1.110	1.115	1.064	1.043

Table 3. Metric Details of **I**, **V**, **VII**, **VIII**, and **IX**

	distances (Å)		
	M−S	C−S	C−O
I $[H_2Dtcat][Ph_4PBr]_2$		1.743(5), 1.773(5)	1.343(7), 1.365(6)
V $[Ni(Dtcat)_2][Ph_4P]_3Br_2$	2.144, [2.147][a]	1.741, [1.742][a]	1.362(8), [1.362(8)][a]
	2.1318(7)−2.1563(7)	1.739(3)−1.746(3)	1.357(3)−1.364(3)
	[2.135(1)−2.157(1)][b]	[1.739(3)−1.746(3)][b]	[1.351(5)−1.368 (5)][b]
VI $Cu(Dtcat)_2][Ph_4P]_3Br_2$	2.175	1.762	1.361(9)
	2.168(1)−2.182(1)	1.753(5)−1.758(5)	1.355(6)−1.368(5)
$[\mathbf{Cu(Dto)_2}]^{-}$ [c]	2.171(7)	1.730 (7)	1.221(6)
VII $[Fe(Dtcat)_2]_2[Ph_4P]_2\cdot 4DMF$	2.225	1.759,	1.381,
	2.2176(8)−2.2318(8)	1.755(3)−1.765(3)	1.371(4)−1.392(3)
VIII $[Ni(Dtoq)_2][Ph_4P]_2$	2.1663(4), 2.1670(4)	1.727(2), 1.728(2)	1.232(2), 1.233(2)
IX $[Cu(Dtoq)_2][Ph_4P]_2$	2.2634(4), 2.2675(4)	1.730(1), 1.724(1)	1.229(2), 1.229(1)
$[\mathbf{Cu(Dto)_2}]^{-2}$ [c]	2.260 (7)	1.703 (5)	1.221(6)

[a] Estimated standard deviations of the least significant digit(s) as calculated by least-squares appear after the (max) and (min) entries. The standard deviations of the averages were taken as the larger of the individual standard deviations or the standard deviation of the mean. [b] From data obtained at 300 K. [c] Dto = the dithiooxalate ligand, average values are given in ref 21.

at different fields from 500 to 5,000 Oe are unambiguously similar. These results preclude the possible admixture at higher temperatures of other magnetic states that may possibly become accessible because of Zeeman effects at 5,000 Oe.

A problem that affects the magnetic data and analyses can be traced to the reactivities of **V** and **VI**. The $S = 1/2$ **V** oxidizes to the diamagnetic **VIII**, and the diamagnetic **VI** oxidizes to the $S = 1/2$ **IX**. An examination of the magnetic properties of **V** and **VI** clearly shows these effects. The latter also are apparent in the electronic spectrum of **V** (Figure 5A) which shows a small amount of the **VIII** impurity at 800 nm and the EPR spectrum of **VI** that shows an impurity EPR signal ($< 2\%$) very likely due to **IX**.

The field dependence of magnetization at 1.9 K gives a saturation value of 0.91 μB up to 7 T. The magnetization curve (Figure 18) is well reproduced by 92% $S = 1/2$ Brillouin function with $g = 2.02(1)$ if we consider this compound containing a diamagnetic Ni(II) coordinated to a ligand radical ($S = 1/2$).

The magnetic properties of **V** are similar to those of the $Ni(tcdt)_2)^{-1}$, $Ni(tdt)_2)^{-1}$, $Ni(bdt)_2)^{-1}$, and $Ni(pdt)_2^{-}$ complexes[23b] at 1.89 BM, 1.79 BM, 1.83 BM, and 1.82 BM, respectively, (tcdt = tetrachlorobenzene dithiol, bdt = benzene dithiol, pdt = tetramethyl benzene dithiol, tdt = toluene dithiol).

On the basis of a DFT calculation of the Ni-dithiolene monoanions, a molecular orbital diagram has been obtained[7a] (Figure 19) that shows the formally Ni(III)

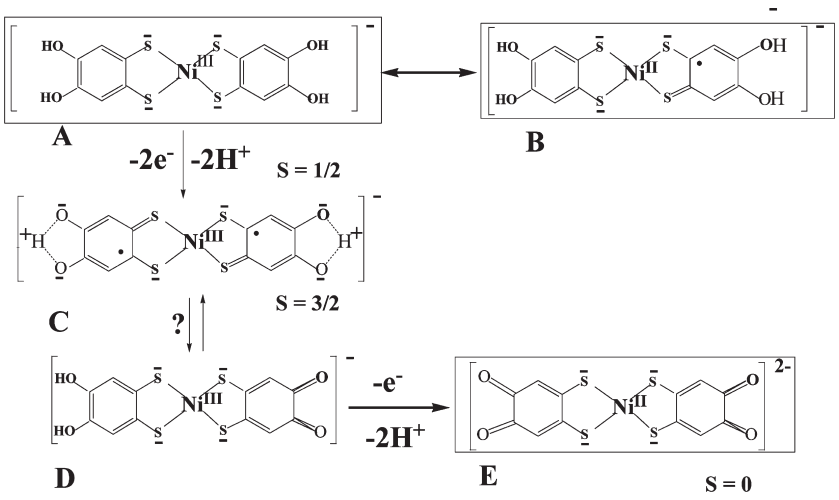

Figure 9. Proposed pathway for the oxidation of the Dtcat complexes to the *o*-quinone., Dtoq, analogues. For M = Ni and Cu the complexes within the brackets have been characterized structurally.

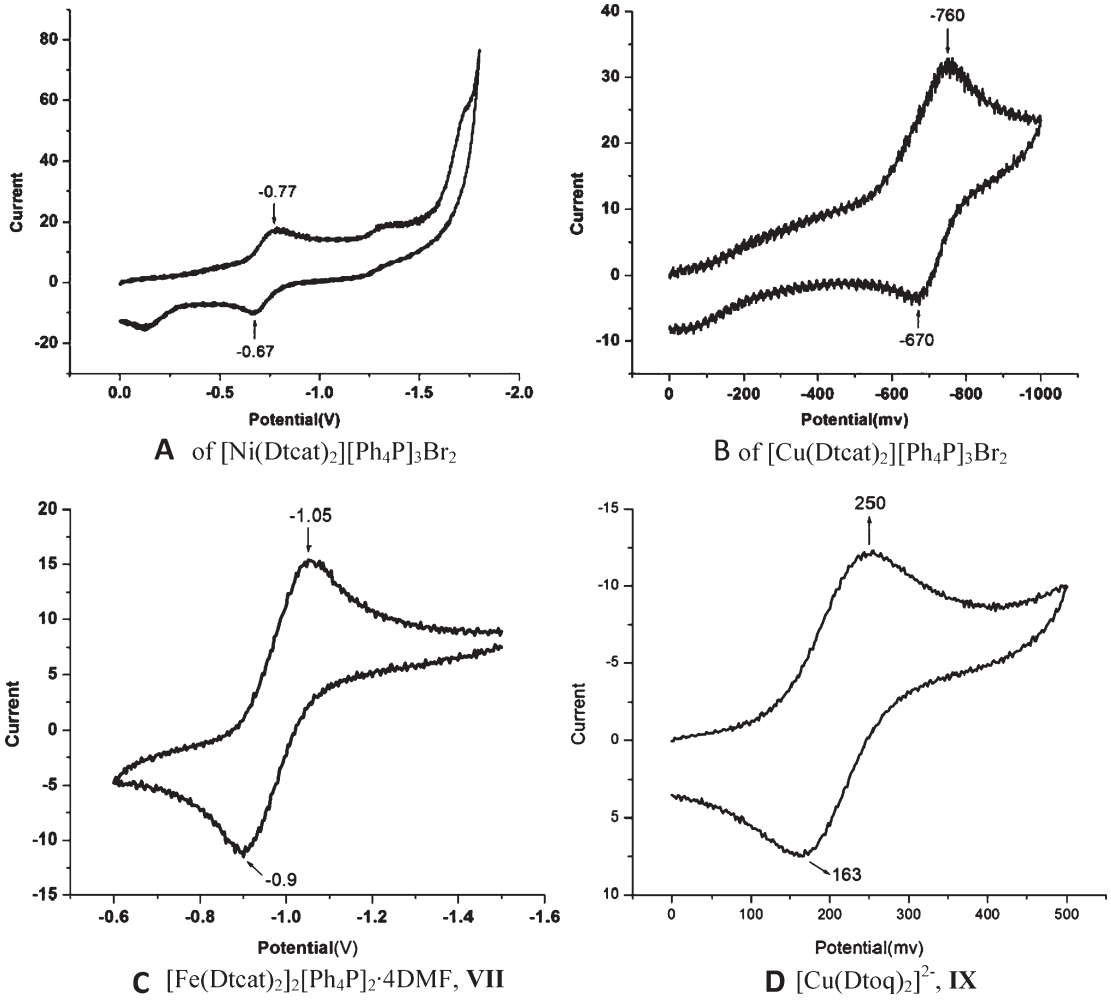

Figure 10. Cyclic voltammograms in DMF of (A) **V**; (B) **VI**; (C) **VII**; and (D) **IX** in CH_3CN solution.

complexes best described as Ni(II) complexes with a half occupied dithiolene ligand highest occupied molecular orbital (HOMO) ($2b_{2g}$). This orbital still has 30% metal (d_{xz}) character.[7a]

This fact also was verified by our DFT calculations (vide infra). Not unlike the other dithiolenes (see above) the ground state for **V** at 1.8 K also is a doublet. Our DFT calculations (vide infra) show a comparable energy level diagram where the **V** monoanion is described as a Ni(II)-dithiolene radical. The very short Ni−S bonds in **V** (Table 2) are similar in length to those in other Ni-dithiolene monoanions (such

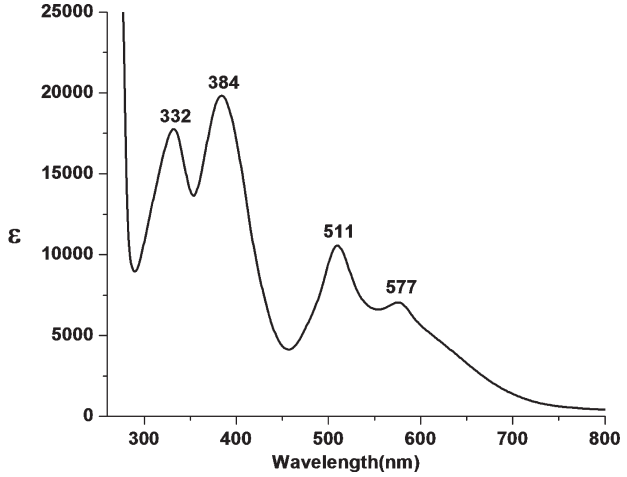

Figure 11. Electronic absorption spectrum $[Fe(Dtcat)_2]_2[Ph_4P]_2 \cdot 4DMF$, in DMF.

as $Ni(S_2C_2(CN)_2)_2]^{-}$ [26,27] and $[Ni(L^{t\text{-}Bu})(L^{t\text{-}Bu}\cdot)_2]^{-}$ [19b] ($L^{t\text{-}Bu}$ = 3,5 di-*tert*-butyl dithiolate at 2.146(1) Å and 2.145(1) Å, respectively) and are 0.02 Å shorter than the Ni−S bond in the $[NiS_2C_2(CN)_2]^{-2}$ dianion at 2.175(1)Å.[18d]

As discussed previously, **V** undergoes oxidation to give as a final product the (structurally characterized) Ni(II)-dithio-orthoquinone product **VIII** (Table 3, Figure 9E) and this oxidation is accelerated in the presence of a base (triethylamine). In this oxidation, an intermediate such as the one shown in Figure 9 is entirely possible and could exist in either an $S = 3/2$ (Figure 9C) or an $S = 1/2$ (Figure 9D) form. We have been unable to intercept intermediates such as 9C or 9D. The EPR spectrum of **V** at 120 K (Figure 4) is rather complex (g values of 2.003, 2.039, 2.136) and similar to that of the $[Ni(L^{t\text{-}Bu})_2]^{-}$ complex[19b] ($L^{t\text{-}Bu}$ = 3,5-di-*tert*-butylbenzodithiolate (2-) ligand) (g = 2.01, 2.04, 2.18). Similar EPR spectra also have been reported for the $\{[Ni[(CN)_2C_2S_2]_2\}^{-1}$ complex.[28]

As previously reported, the Cu dithiolene monoanions, described as Cu(III), d,[8] complexes, are low-spin diamagnetic species. In the temperature range 10−300 K, **VI** is diamagnetic and similar to the $Cu(tdt)_2)^{-}$, $Cu(tcdt)_2)^{-1}$, [23] and $(Cu(Dto)_2)^{-}$ [9b,11] complexes. This characteristic could be considered consistent with a planar, low spin, Cu(III), d,[8] bound to two $[S_2C_6H_2(OH)_2]^{2-}$ ligands. An examination of the C−C bonds in the phenyl rings of the Dtcat ligands (Figure 3), however, shows (Table 4) significant alternations in length consistent with partial ligand oxidation rather than ligand reduction. Indeed, these alternations are quite similar to those found in the structure of **V** for which there is little doubt that ligand oxidation has taken place. In **VII** where minimal intramolecular electron transfer and ligand oxidation is expected the a/c difference (Table 4) is ∼0.01 Å and within 3σ.

On the basis of these data, a bonding description must place a significant contribution of a Cu(II)−S· or even a Cu(I)−S= form to the electronic structure of **VI**. The strong ligand character of the highest occupied MOs in $Cu(tcdt)_2)^{-1}$ has been noted previously,[23] and is clearly evident in the DFT calculations which indicate a deviation from planarity for **VI** (vide infra).

In **VII**, two low spin Fe(III) ($S = 1/2$) sites are weakly coupled antiferromagnetically with a μ_{eff} of 2.81 BM at 270 K and 0.91 BM at 10 K.

The molecular and structural similarities notwithstanding, the electronic structures of **V** and **VI** are different and while the structure of **VI** deviates from planarity (C_2 symmetry) the structure of **V** is planar (C_{2h} symmetry). The reactivity characteristis of **VI** (Figure 20) are similar to those already described for the Ni complex (Figure 9).

Previously we have reported[29] on a possible sulfur-radical-Cu(II) coupling in the structure of the $[Cu_5L_4]^{-}$ anion (where L = dicarbo-*tert*-butoxyethylene-2,2-thioperthiolate). The Cu−S bond length in this compound is quite long at 2.283(9) Å, with a rather large standard deviation, that still places this value outside 3σ from that in **VI** (2.17(1)Å. The Cu−S bond in **VI**, is similar to Cu−S distances in the diamagnetic $[Cu[(CN)_2C_2S_2]_2]^{-1}$ anion[30] at 2.172(4) Å, the $[Cu(Dto)_2]^{-}$ anion at 2.171(7)Å,[31] and the $[Cu(EtDED)_2]^{-}$ anion at 2.195(5)Å[33] (EtDED = 1,1-dicarboethoxy 2,2 ethylene dithiolate).

In the formally Cu(II) complexes $[Cu[(CN)_2C_2S_2]_2]^{-2}$ and $[Cu(Dto)_2]^{-2}$ the Cu−S distances are a full 0.1 Å longer at 2.276(9) Å[30] and 2.270(7) Å,[11b,32] respectively. The oxidation of the $[Cu(Dtoq)_2]^{2-}$ complex (Figure 20E) is electrochemically reversible (Figure 10D). However, the isolated oxidation product is identical to the oxidation product of **V** and does not contain metal. This interesting oxidative degradation of the ligand at present is under investigation.

DFT Calculations. To explore in detail the electronic structures of **V** and **VI** DFT calculations were carried out. These calculations have been done for the anions specified in Figure 13B. See the Experimental Section for details.

Structure optimization (Figure 13B) converged to structures in better than expected agreement with the X-ray crystal structure results (Figure 20). Additional structure optimizations were performed in which four Br^{-} ions were added to the isolated monoanions M-(S2C6H2(OH)2)$^{-}$. It was necessary to include environmental effects by the conductor like screening model (COSMO)[35] to stabilize these highly charged (minus five) ions. Only small geometric changes have been observed. The hydrogen atoms of the OH groups form hydrogen

(26) Fritchie, J. F., Jr. *Acta Crystallogr.* **1966**, *20*, 107.
(27) Weiher, J. F., 1.; Melby, L. R.; Benson, R. E. *J. Am. Chem. Soc.* **1964**, *86*, 4329.
(28) (a) Kirmse, R.; Stach, J.; Dietzsch, W.; Steimecke, G.; Hoyer, E. *Inorg. Chem.* **1980**, *19*, 2699. (b) Maki, A. H.; Edelstein, N.; Davison, A.; Holm, R. H. *J. Am. Chem. Soc.* **1964**, *86*, 4580.
(29) Gammack, R.; Fernandez, V. H.; Schneider, K In *The Bioinorganic Chemistry of Nickel*; Lancaster, J. R., Ed.; VCH Publishers: New York 1988; Chapter 8.
(30) Coucouvanis, D.; Kanodia, S.; Swenson, D.; Chen, S.-J.; Stüdemann, T.; Baenziger, N. C.; Pedelty, R.; Chu, M. *J. Am. Chem. Soc.* **1993**, *115*, 11271–11278.
(31) Forester, J. D.; Zalkin, A.; Templeton, D. H. *Inorg. Chem.* **1964**, *3*, 1507–1515.
(32) Plumlee, K. W.; Hoffman, B. M.; Ibers, J. A.; Soos, Z. G. *J. Chem. Phys.* **1975**, *63*, 1926.
(33) Coucouvanis, D.; Hollander, F. J.; Caffery, M. L. *Inorg. Chem.* **1976**, *15*, 1853.

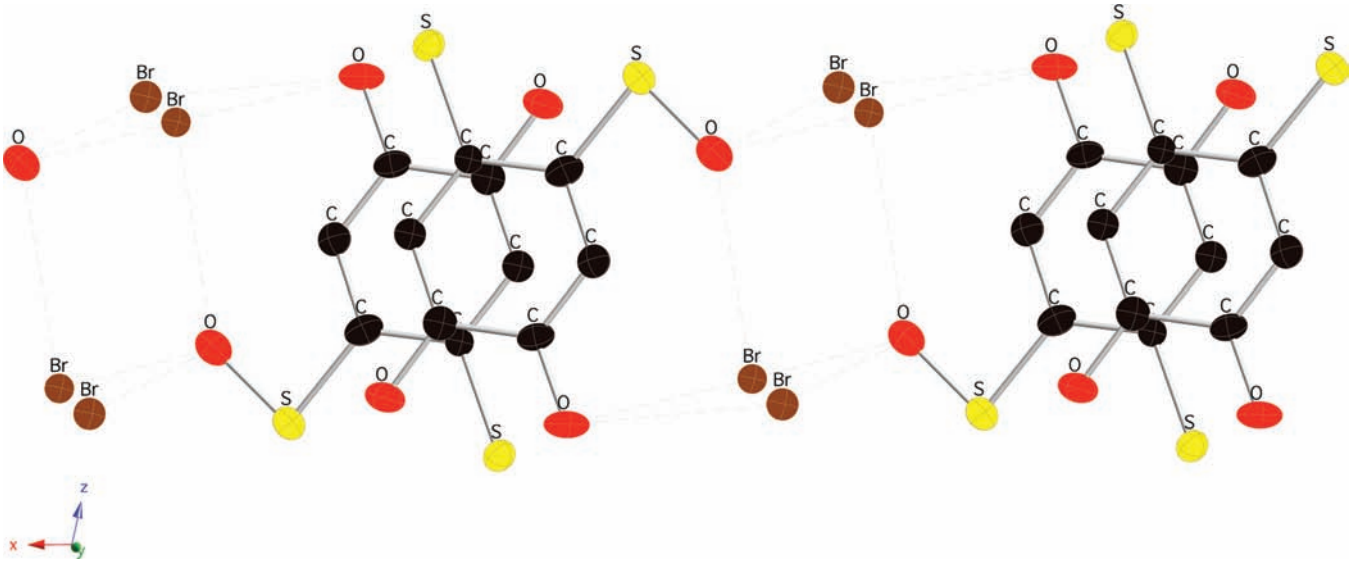

Figure 12. Hydrogen bonding connectivity in the structure of theH_2Dtcat·2Ph_4PBr·H_2O, (**I**). Atom code: Red, Oxygen; Brown, Bromine; Yellow, Sulfur.

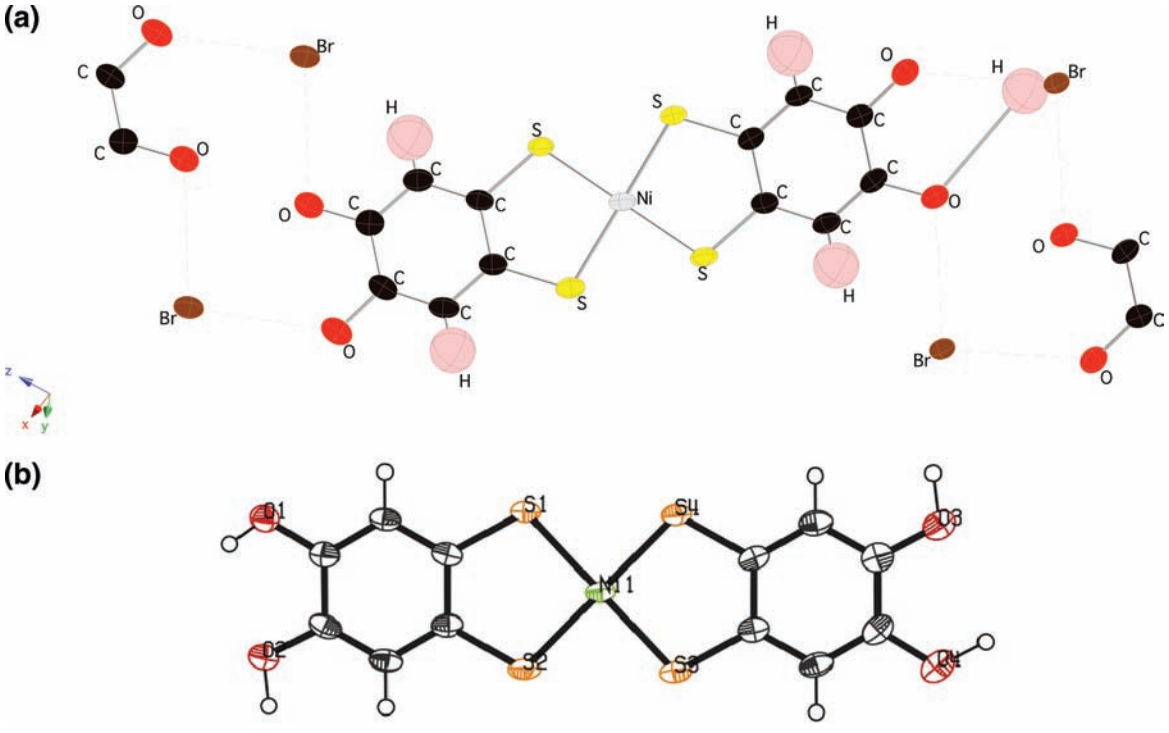

Figure 13. (A) Structure of the $[Ni(Dtcat)_2]^-(Ph_4P)_3Br_2$ complex, (**V**). The Br^- anions (brown spheres) H-bond to planar units to form chains. Red, Oxygen; Brown, Bromine; Yellow, Sulfur; Gray Ni. (B). Thermal ellipsoids represent the 30% probability surfaces. Molecule used in the DFT calculations, C_{2h} planar, C_2 non-planar. The corresponding Cu complex, **VI**, is X-ray isomorphous and isostructural to **V**.

bonds with the Br^- ions, and induce a shortening of the C−O bonds, by two to three pm, which leads to an even better agreement with the experimentally determined structure.

For **V**, three strong bands with oscillator strengths larger than 0.05 have been observed in the energy range below 4.0 eV. A reliable assignment is possible for the lowest transition calculated (at 1.43 eV or 866 nm) and assigned to the intense band at 1015 nm in the experimental spectrum. (Table 1, Figure 5A) It has been characterized as an excitation from the highest doubly occupied orbital, which is a ligand orbital with about 40% sulfur 3p contribution, to the singly occupied molecular orbital (SOMO) which has 27% Ni 3d and 50% sulfur 3p contributions. For **VI** transitions with large oscillator strengths have been found in the calculations at 360 nm (osc. str. 0.59) and 339 nm (osc. str. 0.17). Between those two a third transition is located at 347 nm with a much lower intensity (osc. str. 0.06). The two peaks with higher intensity can be assigned to the two bands observed in the electronic spectrum (at 392 nm and 341 nm, Table 1, Figure 6A).

Molecular electronic structures are conveniently discussed in terms of energetic ordering and charge distribution of occupied MOs as well as resulting total atomic populations. For transition metal compounds

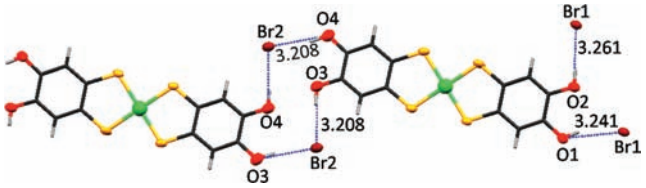

Figure 14. Hydrogen bonded 1-D polymeric chain of complexes **V**. A similar H-bonding pattern with slightly different distances also is present in **VI**.

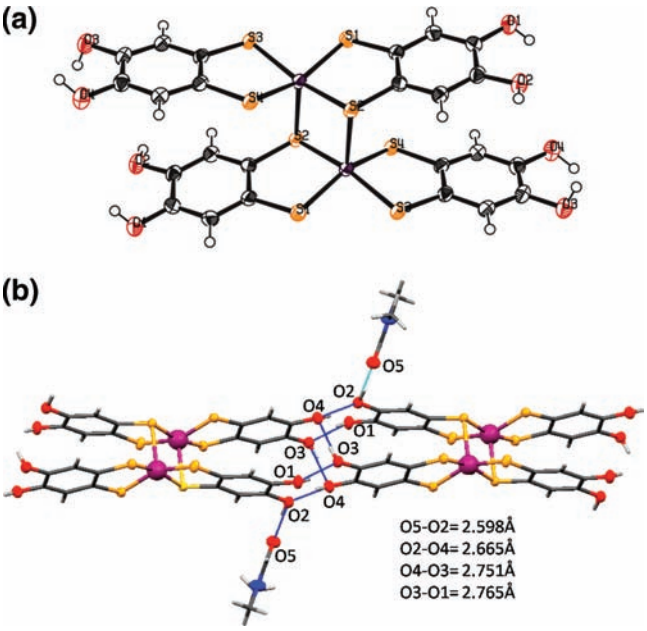

Figure 15. (A) ORTEP plot of the anion in **VII** with thermal ellipsoids drawn at the 30% probability level. (B) Section of the hydrogen bonded 1-D polymeric chain of **VII**.

the (valence) d occupation is of particular interest since this is related to the formal oxidation state of the metal atom. One has to keep in mind, however, that atomic populations are not measurable and thus not computable without some arbitrariness. This ambiguity is reflected in the dependence of results on the DFT functional and the type of population analysis employed. We minimized these uncertainties by presenting and discussing only features which are robust in the sense that a hybrid (B3LYP) and a non-hybrid (TPSS) functional and two population analyses (MPA and NPA) led to very similar results.

Neese, Wieghardt, and co-workers[15] have discussed in detail electronic structures for the complexes depicted in Figure 19. A comparison of their results with those obtained for the structurally similar **V** and **VI** reveals close similarities in many details. The monoanions **V** and **VI** show the same energetic ordering of ligand and metal orbitals as reported[7a,15] for Ni and Cu compounds. The metal d-orbitals are lower in energy than high-lying ligand orbitals and the HOMO or SOMO has just a small metal d contribution, which gives rise to a d spin polarization in case of a single occupation (Figure 19). **V** is a doublet with $S = 1/2$, the 3d spin population (NPA) at Ni is 0.41, which is roughly comparable with the value of 0.31 reported previously[7a] for a Ni dithiolene monoanion; the total d occupations are identical with $3d^{9.03}$.

VI is a closed shell case with $S = 0$, and a Cu d occupation $3d^{9.6}$, again in agreement with results reported in ref 15 for a similar compound.[36] Neese, Wieghardt, and co-workers[15] have concluded that their results are consistent with a formal nd^8 valence electron configuration for M = Ni, Cu although the computed metal d occupation exceeds 8. It was argued that "the charge excess over the formal nd^8 configuration arises from the population of the otherwise unpopulated nd_{xy} orbital (almost single occupation) because of strong σ donation from the b_{1g} ligand fragment orbital."[15] As a consequence of the assumed $3d^8$ occupation, formal oxidation states Ni(II) and Cu(III) were assigned to the metal atoms in $[ML_2]^-$. This interpretation is still acceptable for M = Ni but it encounters difficulties for M = Cu, where the NPA (and MPA) indicate an oxidation state close to Cu(I). This is not only shown by the total d occupations (close to 10) but also by the occupancy of the d_{xy} orbital (formally empty in d^8) of 1.6 (and $3d_{xy}^{1.3}$ for M = Ni), which is most easily characterized as a fully occupied orbital with slight (to medium for Ni) covalent ligand contribution. Since all other 3d orbitals of Cu have an occupation close to 2 (larger than 1.98), they have no direct effect on bonding and structure. The decisive MO is the one with partial d occupation depicted in Figure 21. The MO is (strongly) M−S bonding, which explains the short M−S distances in **V** and **VI**; it further favors the planarity of the complex.

For a Cu(I) case one clearly expects a tetrahedral coordination, and the DFT calculation for planar **VI** (C_{2h}) yields in fact one imaginary frequency for the torsional ligand mode, leading to a distortion to C_2 molecular symmetry with a dihedral angle of 16 degrees between benzene rings (Figure 22). The relaxation from C_{2h} to C_2 is connected with only a minute energy lowering of 2 kJ/mol. The energy gain is too small to influence the structure in the solid since other ionic interactions are clearly more important. It should be noted that the structure determinations of the isostructural **V** and **VI** (and the temperature factors) are not accurate enough to detect the small differences in structure suggested by the DFT calculations.

The Ni compound **V** remains planar with C_{2h} symmetry in agreement with the smaller $3d_{xy}$ occupation and, hence, larger covalent contributions.

Conclusions

An analysis of the spectroscopic and structural characteristics thus far supports B (Figure 9) as a possible structure for **V**. Specifically, structure B (Figure 8) with a Ni(II) coordinated to a radical ligand is supported by the following:

(a) The rather short Ni−S distances (~2.14 Å, Table 2) that are very similar to Ni−S distances in other Ni-dithiolene monoanions.

(34) Kahn, O. *Molecular Magnetism*; Wiley-VCH: New York, 1993.

(35) Klamt, A.; Schuerman, G. *J. Chem. Soc., Perkin Trans. 2* **1993**, 799–805.

(36) The value given for $[Cu(L)_2]^-$ in Table 8 of ref 15 ($3d^{8.92}$) is an obvious misprint. The correct value is $3d^{9.5}$; (Frank Neese, private communication).

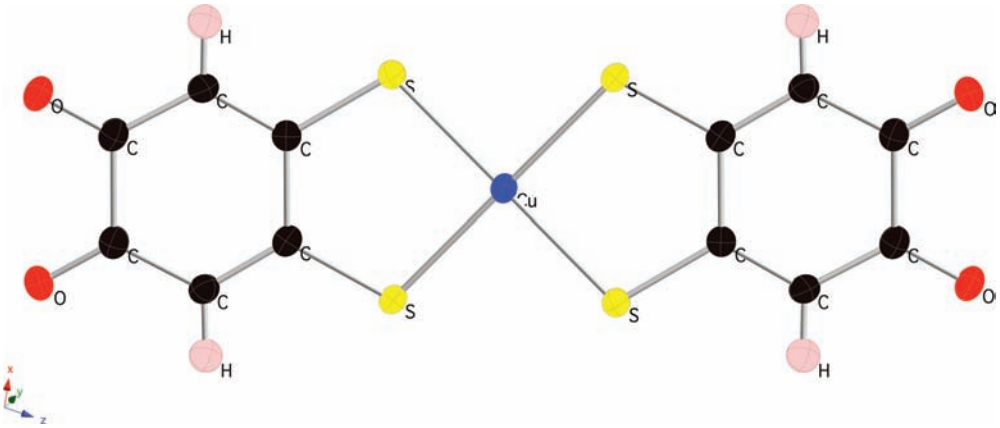

Figure 16. Structure of the X-ray isomorpous $[M(Dtoq)_2]^{2-}$ complexes; M = blue = Ni (**VIII**) or Cu (**IX**); Oxygen = red; Sulfur = yellow.

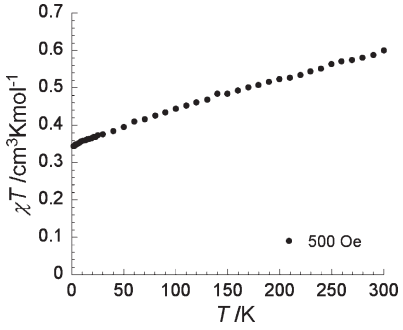

Figure 17. Temperature dependence of susceptibility (χT vs T plot) of **V** under a dc field of 500 Oe. (data corrected for diamagnetism using the diamagnetism of **VI**).

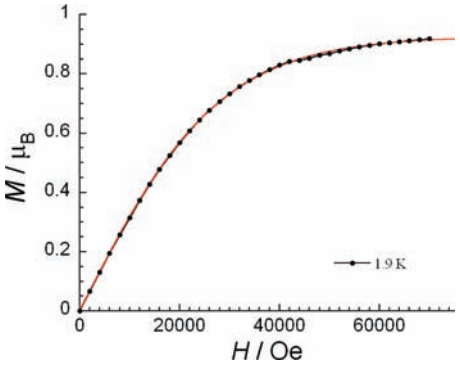

Figure 18. Field dependence of magnetization (M vs H/T plot) at 1.9 K. The solid line is the fit described in the text.

(b) An electronic spectrum that shows the characteristic low energy, high intensity interligand charge transfer band (Figure 5, Table 1).
(c) The magnetic data from 1.8 to 300 K.
(d) The nearly identical structures at 90 K and 300 K.
(e) The long C−O distances in the structure of the ligands, (Table 4) which resemble catechols rather than deprotonated catecholates.

The electronic structure of **VI** is not simply Cu(III) as previously described (vide supra) but is more consistent with appreciable delocalization of electron density out of the copper d_{xy} orbital (fully occupied in d^{10}).

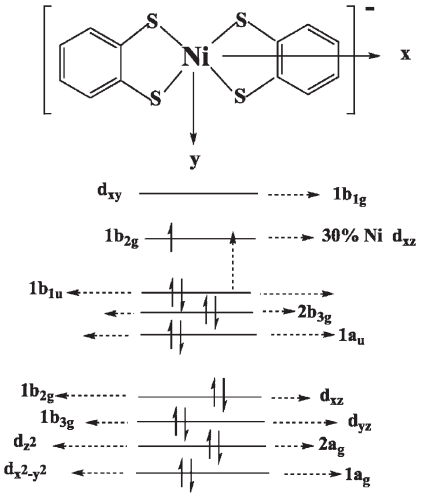

Figure 19. Qualitative energy level diagram obtained[7a] by DFT calculations on the $[Ni(phenyl\text{-}dithiolene)_2]^-$ monoanions.

Experimental Section

Materials and Physical Measurements. All reactions have been performed under Nitrogen atmosphere in a glovebox and standard Shlenck line techniques. All solvents have been distilled and degassed, except DMF that was not

Distilled 4,5-dibromoveratrole, copper(I) butanethiolate are synthesized according to published procedures. IR spectra were collected on a Perkin-Elmer Spectrun BX FT-IR spectrometer and a Nicolet 740 FT-IR spectrometer in KBr pellets. Mass Spectra were collected on a Micromass LCT Time-of-Flight mass spectrometer. Elemental analysis were performed by the Microanalytical Laboratory at the University of Michigan. Electronic spectra collected on a Varian CARY 1E UV−visible spectrometer, and Cyclic Voltammetry experiments were carried out with a Glassy Carbon working and Ag/AgCl reference electrode with 0.1 M Bu_4NPF_6 electrolyte on a EG&G Princeton Potentiostat/Galvanostat model 263A. The redox potentials are reported vs SCE.

Magnetic Measurements. The magnetic susceptibility measurements were performed in the temperature range 300−1.8 K under a dc field of 5000 Oe with the use of a Quantum Design SQUID magnetometer MPMS-XL. The field dependence of magnetization measurements were carried out at 1.9 and 3 K. Measurements were performed on a polycrystalline sample of 15.0 mg. The molecular weight of 1581.15 g/mol was used in the calculations. The magnetic data were corrected by the diamagnetic contribution of the plastic sample holder and diamagnetism

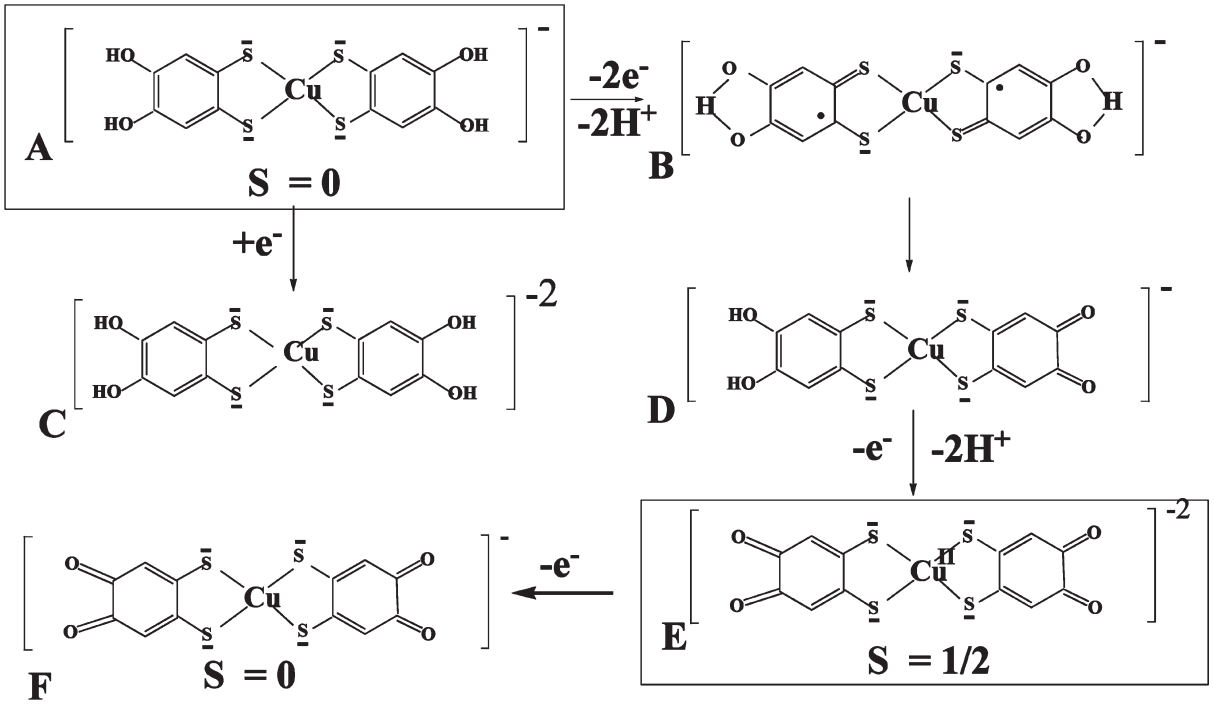

Figure 20. Structure and properties of the $[Cu(DTcat)_2]^-$ and $[Cu(DToq)_2]^{2-}$ complexes. The bracketed molecules have been characterized structurally.

(-9.0×10^{-4} cm^3 mol^{-1}) of the sample measured as a function of temperature, using the diamagnetic isomorphous and isostructural $Cu(Dtcat)_2(Ph_4P)_3Br_2$ complex, **VI**. The χT product at RT is 1.10 cm^3 K mol^{-1}, in good agreement with 90% of the expected value (1.217 cm^3 K mol^{-1}) for three non-interacting $S = 1/2$ spins with $g = 2.08$. With the decrease of temperature, the χT product decreases to reach 0.34 cm^3 K mol^{-1} at 1.8 K (see the semilog plot) indicating the presence of one $S = 1/2$ spin in the system. The behavior shows AF interactions present in the compound. The field dependence of magnetization at 1.9 K gives a saturation value of 0.94 μB up to 7 T. The magnetization curve is well reproduced by 90% $S = 1/2$ Brillouin function with $g = 2.08(1)$.

X-ray Crystallography. Pink colored single crystals of **I** were obtained from MeOH-Ether solution, whereas single crystals of the complexes, **V**, **VI**, **VII**, and **VIII** were obtained by diffusion of diethylether to DMF solutions of these compounds. The intensity data of all the compounds were collected on a Bruker SMART CCD single-crystal X-ray diffractometer at 90 K. The 300 K data for **V** were obtained. Information concerning X-ray data collection and structure refinement of the compounds have been summarized in Table 2.

DFT calculations. DFT calculations have been carried out with the TPSS functional[37] employing a def2-TZVPP basis set[38] which is a triple-ζ type basis augmented by two sets of polarization functions.The RI-J technique (resolution of the identiy approximation for the Coulomb term J) has been used.[39] All structure parameters have been optimized on the basis of redundant internal coordinates.[40] All optimized structures collected in tables were confirmed to be local minima by harmonic frequency calculations. The only exceptions are the calculations on highly charged systems with four additional Br^- ions, sketched in Figure 15, in which environmental effects were included by the conductor like screening model (COSMO).[35] Environmental effects had to be included since these systems would otherwise have positive orbital energies of occupied orbitals. In all other cases ε_{HOMO} was negative. TDDFT (time dependent density functional theory)[41] calculations using the B3LYP functional[42] were carried out to determine electronic excitation energies. As pointed out by a referee, there is a risk that the self-consistent field solver does not converge to the true ground state. Convergence toward saddle points (in the orbital space) would be detected in the TDDFT calculations; this was not observed. For a short hand characterization of the electronic structure population, analyses according to Mulliken (MPA) and Weinhold[43] (natural population analysis, NPA) have been obtained. All calculations have been carried out with TURBOMOLE package version 6.0[44]

Synthesis. 1,2-Bis(*n*-butylthio)-4,5-dimethoxybenzene (II). 4,5-Dibromoveratrole (9.09 g, 30.7 mmol) and copper(I) butanethiolate (10 g, 65.5 mmol) were heated, under reflux, in a mixture of quinoline (50 mL) and pyridine (15 mL) under stirring. The reaction was refluxed for 24 h. During the reflux all the initially undissolved material dissolved to give a dark brown-green solution. After completion of the reflux the mixture was allowed to cool to room temperature and then poured into ice−water containing 75 mL of HCI (3 M). This yielded a dark, gummy solid which was allowed to stand with occasional stirring for 1 h. The water was decanted and washed with CH_2Cl_2 (100 mL). The extract was then added to the gummy residue and stirred for 10 min. The gum was extracted a further four times with portions of CH_2Cl_2 (25 mL), until the extract was colorless.

(37) Tao, J.; Perdew, J. P.; Staroverov, V. N.; Scuseria, G. E. *Phys. Rev. Lett.* **2003**, *91*, 146401.
(38) (a) Weigend, F.; Ahlrichs, R. *Phys. Chem. Chem. Phys.* **2005**, *7*, 3297. (b) Weigend, F. *Phys. Chem. Chem. Phys.* **2006**, *8*, 1057.
(39) (a) Eichkorn, K.; Treutler, O.; Öhm, H.; Häser, M.; Ahlrichs, R. *Chem. Phys. Lett.* **1995**, *240*, 283. (b) Sierka, M.; Hogekamp, A.; Ahlrichs, R. *J. Chem. Phys.* **2003**, *118*, 9136.
(40) von Arnim, M.; Ahlrichs, R. *J. Chem. Phys.* **2003**, *111*, 9183.
(41) (a) Casida, M. E. In *Recent Advances in Density functional methods*; Chong, D. P., Ed.; World Scientific: Singapore, 1995; Vol. 1 of Recent Advances in Computational Chemistry, p 155. (b) Bauernschmitt, R.; Ahlrichs, R. *Chem. Phys. Lett.* **1996**, *256*, 454. (c) Bauernschmitt, R.; Häser, M.; Treutler, O.; Ahlrichs, R. *Chem. Phys. Lett.* **1997**, *264*, 573.
(42) (a) Becke, A. D. *J. Chem. Phys.* **1993**, *98*, 5648–5652. (b) Lee, C.; Yang, W.; Parr, R. G. *Phys. Rev.* **1988**, *B37*, 785–789.
(43) Reed, A. E.; Weinstock, R. B.; Weinhold, F. *J. Chem. Phys.* **1985**, *83*, 735.
(44) *TURBOMOLE*, version 6.0; TURBOMOLE GmbH: Karlsruhe, Germany, 2008; www.turbomole.com.

Table 4. Comparison of Phenyl Ring Structural Data in **V**, $\mathbf{V}_{300K}$, **VI**, **VIII**, and **IX**

	$[Ni(Dtcat)_2]^-$				$[Cu(Dtcat)_2]^-$		$[Fe(Dtcat)_2]_2^{2-}$
	V				**VI**		**VII**
	90 K	300 K	DFT	DFT with Br^-	90 K	DFT	90 K
a	1.369(4)[a]	1.372(5)	1.388	1.425	1.374(5)	1.390	1.382(4)
			1.386			1.389	
b	1.405(4)	1.412(5)	1.411	1.394	1.404(5)	1.400	1.393(4)
c	1.394(6)	1.396(7)	1.411	1.409	1.386(9)	1.405	1.395(4)
				1.410			
d	1.405(5)	1.405(5)	1.418	141.4	1.398(5)	1.405	1.398(3)
e	1.366(4)	1.362(8)	1.383	1.365	1.361(9)	1.386	1.387 (3)
			1.396	1.368		1.400	1.375
f	1.741(5)	1.742(4)	1.745	1.755	1.762(11)	1.763	1.760(2)
			1.746	1.755		1.762	1.757
Ni−S	2.156(1)	2.156(1)	2.173	2.168,			
	2.133(1)	2.137(3)	2.176	2.169			
Cu−S					2.182(1)	2.211	
					2.168(1)	2.209	
Fe−S							2.225(7)

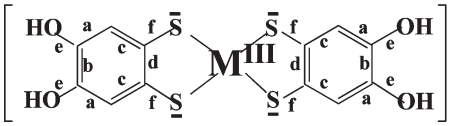

	$[Ni(Dtoq)_2]^{2-}$		$[Cu(Dtoq)_2]^{2-}$	
	VIII		**IX**	
	90 K	DFT	90 K	DFT
a	1.439(5)[a]	1.433	1.440(3)	1.438
b	1.543(4)	1.543	1.544(3)	1.551
c	1.365(3)	1.378	1.366(3)	1.380
d	1.481(3)	1.494	1.496(4)	1.494
e	1.233(3)	1.245	1.229(3)	1.243
f	1.727(2)	1.729	1.727(2)	1.728
Ni(Cu)−S	2.166(1) 2.167	2.182	2.263(1), 2.268(1)	2.303, 2.289

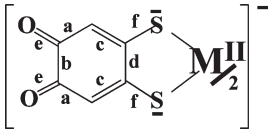

[a] Estimated standard deviations of the least significant digit(s) as calculated by least-squares appear after the (max) and (min) entries. The standard deviations of the averages were taken as the larger of the individual standard deviations or the standard deviation of the mean.

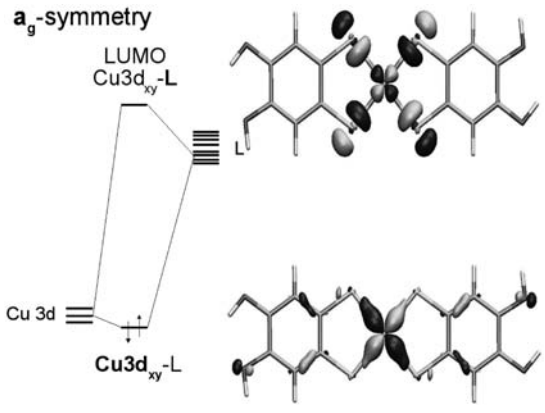

Figure 21. Kohn−Sham MO $36a_g$ and $42a_g$ of VI in C_{2h} symmetry. The d_{xy} orbital of the metal has the strongest interaction with ligand orbitals and $36a_g$ is the lowest energy MO with a large d contribution. The corresponding antibonding partner $42a_g$ is unoccupied and has only a small d contribution. For the remaining d orbitals the bonding and antibonding M−L combinations are occupied.

The red brown dichloromethane solution was washed with portions of water (200 mL), 1 M hydrochloric acid (3 × 30 mL), water (200 mL), 1 M NH_4OH (2 × 30 mL), and, finally, water (2 × 200 mL). The dichloromethane layer was dried over $MgSO_4$, and the solvent evaporated to give a dark red oil. On standing the oil crystallized to give off a white crystalline product. Yield about 55%. Mp 52−55. NMR ($CDCl_3$,): ^1H (300 MHz), 6.9 (s, 2H), 3.88 (s, 6 H), 2.86 (br, 4 H), 1.62 (m, 4H), 1.45 (m, 4H), and 0.92 (t, 6H).

Dilithium 4,5-dimethoxybenzene-1,2-dithiolate (III). 1,2-Bis-(*n*-butylthio)-4,5-dimethoxybenzene (4 g, 12.8 mmol) was dissolved in a minimum quantity of dry tetrahydrofuran (thf), used as a cosolvent, and placed in a three-necked, round-bottom flask which had previously been flushed with dinitrogen. One neck of the flask was connected to the dinitrogen supply, one to an ammonia cylinder, and the third to a bubbler through a dry ice-acetone condenser. A slow stream of ammonia gas was admitted to the reaction vessel until about 10 cm^3 of liquid ammonia had condensed. At this point the ammonia flow was stopped, but a slow stream of dinitrogen was maintained for the duration of the experiment. Lithium metal (at least 5 equivalents) was added portion wise through the ammonia inlet, the blue color being

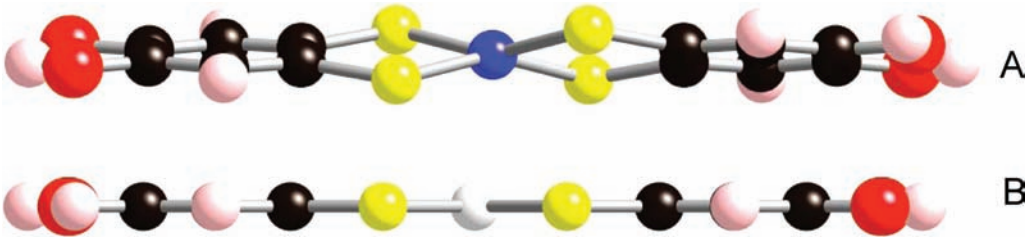

Figure 22. Side on view of the DFT structure optimized **VI** (A) and **V** (B).

allowed to discharge between additions. When the blue color of lithium in ammonia persisted, unabated, for over 30 min, the reaction was adjudged to be complete. An excess of solid NH_4Cl was then added to destroy the excess of lithium. The rate of flow of the dinitrogen gas was then increased, and the liquid ammonia allowed to evaporate. The residual thf solvent was evaporated under reduced pressure to leave an off-white solid containing the required dilithium salt which was used to prepare tetraphenylphosphonium salt without further characterization.

Bis-tetraphenylphosphonium 4,5-Dimethoxybenzene-1,2-dithiolate (IV). To the above enclosed round bottomed flask under ice−water, 100 mL water was passed through a cannula which was degassed with Nitrogen overnight and stirred for 10 min and then filtered into a 500 mL round bottomed flask containing PPh_4Br (10 g, 23.8 mmol) in 250 mL of warm water which was degassed and then stirred for 30 min to give a yellow solid of diphosphonium salt. Then the above precipitate was filtered and washed with ether and dried under vacuum. Yield about 6 g. NMR (DMSO-d^6): ^{1}H (300 MHz), 8−7.6 (m, 42H), 3.6(s, 6H). MS: (ESI+)m/z ; 339. (ESI−)m/z ; 201, 186, 171, 156.

Bis-tetraphenylphosphoniumbromide 4,5-Dihydroxybenzene-1,2-dithiol (I). To the dichloromethane solution (15 mL) of Bis-tetraphenylphosphonium 4,5-Dimethoxybenzene-1,2-dithiolate (6 g, 7.05 mmol) at inert atmosphere using N_2 inlet, BBr_3 (1:5 equivalent) was added to the above solution and stirred for 24 h. It was observed that after addition of BBr_3 the solution color was changed from yellow green to blue in color. After 24 h, 10 mL of dry methanol was used to quench excess BBr_3. Then the solution was dried under vacuum to give some pink colored oil which again was treated with methanol and dried without exposing to air. Then the pink oil was taken inside glovebox and dissolved with minium MeOH (10 mL), and ether was added until a permanent cloudiness appears. After 2 days it gives pink crystalline materials. Yield = 58%. MW = 1030.84. Anal. Calcd for $C_{54}H_{48}Br_2O_3P_2S_2$: C, 62.92; H, 4.69. Found: C, 62.86; H, 4.38. IR(cm^{-1}): 3050(m), 1583(m), 1482(s), 1434(vs), 1314(w), 1185(w), 1107(vs), 994(m), 754(m), 723(vs), 688(vs), 524(vs). NMR (DMSO): ^{1}H (300 MHz), 8−7.6 (m, 42H). MS: (ESI+) m/z; 339.1. MS: (ESI−)m/z; 173, 253.

[(Dtcat)$_2$Ni][Ph$_4$P]$_3$Br$_2$ (V). To the dmf solution of ligand (1.4 g, 1.38 mmol taken in 10 mL of dmf), $Ni(OAC)_2\cdot 4H_2O$ (0.171 g, 0.69 mmol taken in 5 mL of dmf) was added dropwise under stirring condition to give a brown colored solution and stirred for another 1 h. Then the above mixture was filtered and layered with 30 mL of ether to give a brown crystalline material. Yield = (1 g, 45.83%). MW = 1581.12. Anal. Calcd for $C_{84}H_{68}Br_2NiO_4P_3S_4$: C, 63.81; H, 4.33; S, 8.11. Br, 10.24. Found: C, 63.82; H, 4.31; S, 8.13. Br, 10.06 IR(cm^{-1}): 3424(m), 3047(s), 1660(m), 1583(m), 1539(s), 1476(m), 1433(s), 1396(s), 1336(w), 1310(w), 1247(vs), 1196(s), 1166(m),1146(m), 1104(vs), 1070(s), 994(m), 868(w), 798(w), 753(m), 721(vs), 688(vs), 632(w), 528(vs), 454(w), 370(m). NMR (DMSO): ^{1}H (300 MHz), 8.1−7.7 (m, 42H). MS: (ESI+)m/z; 339. (ESI−)m/z; 401.8, 385.8. UV−vis (DMF): 372, 314 nm.

[(Dtcat)$_2$Cu][Ph$_4$P]$_3$Br$_2$ (VI). To the dmf solution of ligand (1 g, 0.99 mmol taken in 10 mL of dmf), $Cu(OAC)_2\cdot 2H_2O$ (0.01 g, 0.5 mmol taken in 5 mL of dmf) was added dropwise under stirring condition to give a brown green solution and stirring continued for another 1 h. Then the above mixture was filtered and layered with 30 mL of ether to give a green crystalline material. Yield = (0.64 g, 40.73%) MW = 1586.98. Anal. Calcd for $C_{84}H_{68}Br_2CuO_4P_3S_4$: C; 63.61, H,4.32; S, 8.09. Found; 63.2, 4.12, S 7.92. IR: 3078(m), 3050(m), 1584(m), 1481(s), 1435(vs), 1312(m), 1182(m), 1164(w), 1105(vs), 1027(w), 994(s), 849(w), 759(s), 724(vs), 688(vs), 528(vs), 445(w), 454(w), 368(m). NMR (DMSO-d^6): ^{1}H (300 MHz), 8.1−7.7 (m, 42H). UV−vis (DMF): 392, 341 nm. MS: (ESI+) m/z; 339. (ESI−) m/z; 406.7, 325, 304, 260, 232.8, 227.

[(Dtcat)$_2$Fe]$_2$[Ph$_4$P]$_2\cdot$4DMF (VII). To the dmf solution of ligand (0.8 g, 0.79 mmol taken in 10 mL of dmf), $Fe(OAC)_2$ (0.068 g, 0.39 mmol taken in 5 mL of dmf) was added dropwise under stirring condition to give a deep violet color and stirring continued for 1 h. Then the above mixture was filtered and layered with 30 mL of ether to give a deep violet crystalline material. Yield = 50%. MW = 1771.75. Anal. Calcd for $C_{84}H_{84}Fe_2N_4O_{12}P_2S_8$: C, 56.94; H, 4.78. Found: C, 56.12; H, 4.44. IR: 3409(m), 3247(m), 3047(m), 2915(w), 1653(vs), 1583(m), 1480(m), 1428(vs), 1303(m), 1255(vs), 1192(m), 1163(m), 1104(s), 993(w), 960(w), 849(w), 787(w), 753(s), 720-(vs), 687(m), 529(vs), 440(w), 355(s). UV−vis(DMF): 579, 510, 384, 331, 265. MS: (ESI+)m/z; 339. (ESI−)m/z; 398, 382, 224, 182, 155.

[(Dtoq)$_2$Ni][Ph$_4$P]$_2$ (VIII). Method A. The DMF solution of complex **V** (0.35 g, 0.22 mmol taken in 10 mL of DMF) was stirred in air for 24 h. During this period the color of the solution changed from brown to green. Then the above mixture was filtered and layered with 20 mL of ether to give a green crystalline material. [Note: If the same reaction is done in presence of 4 equiv of base, oxidation is faster and goes to completion within 2 h] Yield = 52%. M_w = 1077.89. Anal. Calcd for $C_{60}H_{44}NiO_4P_2S_4$: C, 66.86; H, 4.11. Found: C, 66.68, H, 4.04. IR: 3424(w), 3047(w), 1587(vs), 1576(s), 1476(vs), 1432(s), 1317(s), 1281(m), 1159(w), 1104(s), 1048(vs), 993(m), 816(w), 761(w), 720(vs), 683(m), 617(m), 525(s). MS: (ESI+)m/z; 339. (ESI−)m/z; 398.7, 227.8, 198.9, 169.9, 141.9.

Method B. To the acetonitrile solution of Complex **V** (0.25 g, 0.16 mmol in 10 mL), in situ generated ylide of *N*-chlorosuccinimide (NCS) (0.0423 g, 0.32 mmol) and Me_2S (0.024 mL, 0.32 mmol) in 5 mL of acetonitrile was added dropwise under stirring condition in an inert atmosphere. Then to the above mixture 0.1 mL of triethylamine was added and stirred for 1 h. Then the above green solution was filtered to remove some insoluble precipitate and layered with 20 mL of diethyl ether to give a green crystalline material of **VIII** in 55% yield.

[(Dtoq)$_2$Cu][Ph$_4$P]$_2$ (IX). Method A. The dmf solution of complex **VI** (0.3 g, 0.18 mmol taken in 10 mL of dmf) was stirred in air for 24 h. During this period the color of the solution changed from green to brown. Then the above mixture was filtered and layered with 20 mL of ether to give a dark colored crystalline material. [Note: If the same reaction is done in presence of 4 equiv of base (Et_3N), oxidation is faster and goes to completion within 30 min] Yield = 60%. M_w =1082.75. Anal. Calcd. for $C_{60}H_{44}CuO_4P_2S_4$: C, 66.56; H, 4.10. Found: C,

66.10; H, 4.12. IR: 3424(w), 3047(w), 1598(vs), 1480(vs), 1435(s), 1310(vs), 1277(m), 1159(w), 1104(s), 1037(vs), 993(m), 823(m), 761(m), 720(vs), 683(m), 610(m), 521(s). MS: (ESI+)*m*/*z*; 339. (ESI−)*m*/*z*; 402.7, 232.8, 204.8, 169.9, 141.9.

Method B. To the acetonitrile solution of Complex **VI** (0.3 g, 0.18 mmol in 10 mL), in situ generated ylide of *N*-chlorosuccinimide (NCS) (0.05 g, 0.38 mmol) and Me_2S (0.028 mL, 0.36 mmol) in 5 mL of acetonitrile was added dropwise under stirring condition in an inert atmosphere. Then to the above mixture 0.12 mL of triethylamine was added and stirred for 1 h. Then the above brown solution was filtered to remove some insoluble precipitate and layered with 20 mL of diethyl ether to give a green crystalline material of **IX** in 61% yield.

Reaction of VIII with $[Cp_2Fe]PF_6$. To the DMF solution of Complex **VIII** (0.25 g, 0.23 mmol in 10 mL), ferrocenium hexafluorophosphate (0.076 g, 0.23 mmol) was added in small portions under stirring condition in an inert atmosphere. It was observed that the color becomes brown-violet from brown and stirred for 1 h. Then the above solution was filtered and layered with diethyl ether to give a red-brown precipitate. Considering formula $C_{12}S_3O_4H_4 \cdot$DMF, Yield = 52%. M_w = 381.45. Anal. Calcd. for $C_{15}H_{11}NO_5S_3$: C, 47.23; H, 2.91. Found: C, 47.68; H, 3.60. IR: 3409(w), 1649(vs), 1491(vs), 1432(s), 1380(vs), 1247(m), 1107(m), 1059(m), 857(m), 835(m), 753(w), 720(w), 687(w), 635(w), 554(w), 525(w).

Similar observations were found for reaction of **IX** with $[Cp_2Fe]PF_6$, which shows similar analytical data (IR and elemental analysis; C, 47.23; H, 2.91).

Acknowledgment. The authors acknowledge support of this research by a National Institutes of Health Grant F017657-055442.

Supporting Information Available: Crystallographic data, CIFs, syntheses, and characterization of ligand and complexes. This material is available free of charge via the Internet at http://pubs.acs.org.